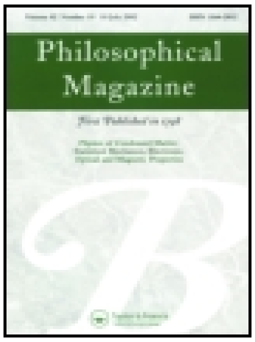

Philosophical Magazine Part B

ISSN: 1364-2812 (Print) 1463-6417 (Online) Journal homepage: http://www.tandfonline.com/loi/tphb20

Ferromagnetism in the $UCo_{1-x}Ru_xAl$ quasiternary intermetallics

A. V. Andreev , L. Havela , V. Sechovsk , M. I. Bartashevich , J. ŠEbek , R. V. Dremov & I. K. Kozlovskaya

To cite this article: A. V. Andreev , L. Havela , V. Sechovsk , M. I. Bartashevich , J. ŠEbek , R. V. Dremov & I. K. Kozlovskaya (1997) Ferromagnetism in the $UCo_{1-x}Ru_xAl$ quasiternary intermetallics, Philosophical Magazine Part B, 75:6, 827-844, DOI: 10.1080/13642819708205710

To link to this article: http://dx.doi.org/10.1080/13642819708205710

PHILOSOPHICAL MAGAZINE B, 1997, VOL. 75, NO. 6, 827–844

Ferromagnetism in the $UCo_{1-x}Ru_xAl$ quasiternary intermetallics

By A. V. ANDREEV†‡, L. HAVELA§, V. SECHOVSKÝ§, M. I. BARTASHEVICH‡, J. ŠEBEK†, R. V. DREMOV† and I. K. KOZLOVSKAYA†

†Institute of Physics, Academy of Sciences, Na Slovance 2, 18040 Prague 8, Czech Republic
‡Permanent Magnets Laboratory, Ural State University, 620083 Ekaterinburg, Russia
§Department of Metal Physics, Charles University, Ke Karlovu 5, 12116 Prague 2, Czech Republic

[*Received 20 November 1996 and accepted 19 December 1996*]

ABSTRACT

We report the structure and magnetic investigations of the quasiternary $UCo_{1-x}Ru_xAl$ compounds crystallizing in the hexagonal structure of the ZrNiAl type. A large deviation from linearity is observed in the concentration dependence of lattice parameters, positive for *a* and negative for *c*, whereas the unit-cell volume *V* obeys Vegard's law satisfactorily. The nonlinearity is explained by a preferential occupation by the Co and Ru atoms of the two non-equivalent positions of the transition metal in the lattice. Although UCoAl and URuAl are paramagnetic down to low temperatures, ferromagnetism is observed in a wide concentration range of quasiternary solid solutions $UCo_{1-x}Ru_xAl$. Both the Curie temperature and the spontaneous magnetization reach their maximum values of 60 K and $0{\cdot}6\mu_B$ (formula unit)$^{-1}$ respectively in $UCo_{0{\cdot}7}Ru_{0{\cdot}3}Al$. The samples in the Ru concentration range $0{\cdot}5 \leqslant x \leqslant 0{\cdot}7$ exhibit a second phase transition in the ordered state, indicated by anomalies in temperature dependence of both the spontaneous magnetization and the ac susceptibility. The development of magnetism is discussed in the framework of the anisotropic 5f–ligand hybridization and the direction dependent exchange interactions mediated by it.

§ 1. INTRODUCTION

The uranium intermetallics UTX with the hexagonal crystal structure of the ZrNiAl type (space group $P\bar{6}m2$; three formula units (f.u.'s) per unit cell) form one of the largest isostructural groups of uranium compounds (T is a late transition metal from the 3d, 4d or 5d series, X is a p metal of the group III, IV or V of the periodic table). Magnetic and other electronic properties of these materials have been systematically studied (see Andreev and Bartashevich (1986), Palstra (1986), Sechovsky *et al.* (1986), Sechovsky and Havela (1988), and references therein).

The crystal structure is schematically shown in fig. 1. All U atoms have equivalent positions, as well as atoms of the p-metal X, whereas T atoms occupy two non-equivalent positions T_1 and T_2 in the ratio 1 : 2. The lattice is built up of two types of basal-plane layer $(3U + T_1)$ and $(3X + 2T_2)$ alternating along the *c* axis. Each U atom has four U nearest neighbours within the basal plane and two other neighbour U atoms somewhat more apart along the *c* axis.

Fig. 1

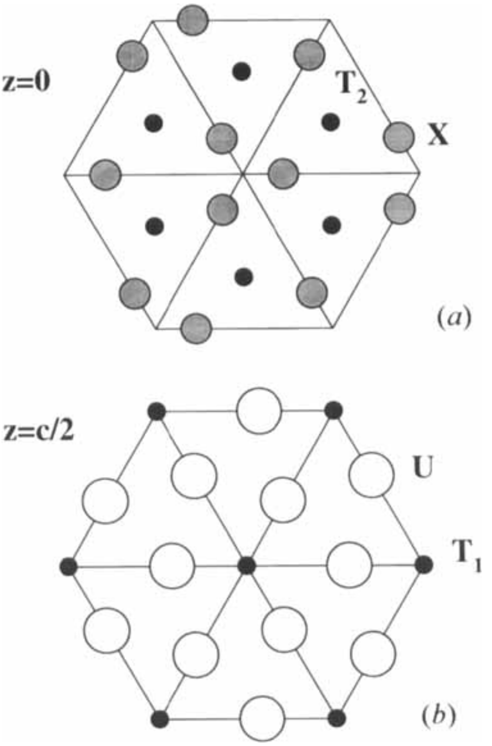

Hexagonal crystal structure of the ZrNiAl type.

The U ground-state magnetic moment in compounds of this family varies from 0 to $1{\cdot}6\mu_B$, depending mainly on the degree of itinerancy of the 5f electrons of U, which may be due to overlapping 5f wavefunctions centred on neighbouring U atoms and hybridization of the 5f states with the valence electron states of ligands (5f–ligand hybridization). Then, although the non-U atoms do not contribute much to the magnetic moment itself, they may affect the magnetic properties considerably by influencing the 5f-electron states. All the compounds, irrespective of the ground state, which can be ferromagnetic (the typical representatives are UCoGa, UCoSn and URhAl), antiferromagnetic (UNiAl and UPdIn) or paramagnetic (UCoAl, URuAl and URuGa), exhibit a huge uniaxial magnetic anisotropy.

The variety of magnetic ground states in the UTX family may be roughly systematized considering the dependence of the strength of the 5f–ligand hybridization on the type and occupation of the ligand valence states and the size of the ligand atoms. The dual role of the hybridization in magnetism involves formation of magnetic moments on the one hand and mediation of exchange interactions on the other hand.

UCoAl and URuAl represent paramagnets with spin fluctuation features. Magnetic properties of both compounds were studied in detail on single crystals. They do not order magnetically (at least down 20 mK) although the high-temperature magnetic susceptibility exhibits Curie–Weiss behaviour (URuAl above 70 K and UCoAl above 40 K). Both compounds are highly anisotropic paramagnets with the maximum susceptibility χ_c along the *c* axis (Sechovsky *et al.* 1986, Veenhuizen *et al.* 1988). A broad maximum on the $\chi_c(T)$ curve at 50 K, an electrical resistivity anomaly below 70 K, and a noticeable S-shape of the *c*-axis magnetization curve measured at 4·2 K are arguments to classify URuAl as a spin fluctuation system (Havela *et al.* 1985, Sechovsky *et al.* 1986, Sechovsky and Havela 1988, Veenhuizen *et al.* 1988). The 'metamagnetic transition' takes place over rather a wide magnetic field interval (about 20–40 T) and the related change in the magnetic moment is rather small ($\Delta\mu_U \approx 0{\cdot}10\mu_B$), but clearly observable (Sechovsky *et al.* 1992). Also UCoAl exhibits a maximum of the $\chi_c(T)$ curve, now at 16 K, and a metamagnetic transition, but the transition field B_c is extremely low (about 1 T) and the transition, although not very sharp, is much more pronouced ($\Delta\mu_U \approx 0{\cdot}25\mu_B$). In the first study of UCoAl (Andreev *et al.* 1985), the antiferromagnetic ground state was proposed in analogy with the isostructural compound UNiAl (Zogal *et al.* 1984). However, the temperature dependence of the specific heat has no anomaly indicative of magnetic ordering (as well as temperature dependences of the electrical resistivity and the lattice parameters *a* and *c*) and thus it has been concluded that the metamagnetic transition occurs from paramagnetic ground state (Sechovsky *et al.* 1986). This conclusion has been corroborated by the *ab-initio* electron structure calculations made by Eriksson *et al.* (1989) and partly by polarized-neutron diffraction studies (Wulff *et al.* 1990).

It was natural to expect that the ground state of the quasiternary solid solutions between these two paramagnetic compounds, $UCo_{1-x}Ru_xAl$, would be paramagnetic throughout. When substituting Ru for Co, a gradual increase in the transition field B_c, a broadening of the metamagnetic transition and a decrease in $\Delta\mu_U$ could have been predicted. However, a pilot study has revealed relatively strong ferromagnetism in $UCo_{0{\cdot}9}Ru_{0{\cdot}1}Al$ with a spontaneous moment of $0{\cdot}5\mu_B$ fu^{-1} and Curie temperature $T_C = 43$ K (Andreev *et al.* 1995a). In the present paper, the fundamental magnetic properties of the whole system $UCo_{1-x}Ru_xAl$ are investigated.

§ 2. EXPERIMENTAL DETAILS

The alloys with nominal compositions $UCo_{1-x}Ru_xAl$ were prepared by melting the corresponding amounts of the elemental components (purity of U, 99·8%; purity of other metals, 99·99%) in an arc furnace on a water-cooled Cu bottom under a protective Ar atmosphere. The ingots (of about 3 g mass) were turned several times and remelted to assure good homogeneity. They were subsequently wrapped in a Ta foil and annealed in vacuum at 750°C in a sealed quartz tube for 1 week. The phase composition of the alloys and lattice parameters were determined by standard X-ray diffractometry. The magnetic properties were measured both on annealed and as-cast samples, and no visible differences were found.

The magnetization was measured by the induction method in pulsed magnetic fields up to 10 T on powder samples at 4·2 K. The randomly oriented powder particles were fixed by a diluted acetone glue to avoid an alignment of the particles in high magnetic fields. The magnetization of several samples was also measured with a superconducting quantum interference device magnetometer in a superconducting coil up to 5 T and $T \geqslant 2$ K. The dc magnetic susceptibility of several compounds was measured by the Faraday balance in a superconducting magnet in fields up to 2 T. Curie temperatures were determined by ac susceptibility measurements.

§ 3. RESULTS AND DISCUSSION

3.1. *Crystal structure*

The X-ray phase analysis showed that all the alloys studied are close to a single phase with the ZrNiAl structure. The composition of the representative alloy $UCo_{0\cdot33}Ru_{0\cdot67}Al$ was checked also by microprobe analysis. This compound with a Co : Ru ratio of 1 : 2 is chosen for a more detailed further study of crystal and magnetic structures for the reasons given below. A few per cent of spurious U-rich and an Al-rich phases have been observed. The composition of the U-rich phase (with 87 at.% U) corresponds well to the well known paramagnetic U_6Co with small amounts of Al and Ru. The composition of the Al-rich phase is found to be $U_2CoRu_2Al_5$. The formation of any $U_2T_3Al_5$ phase has not been reported so far (according to our best knowledge), but Si and Ge (instead of Al) analogues have already been described (see Morozkin and Seropegin (1996), and references therein). The temperature dependence of the ac susceptibility of a separately prepared sample with $U_2CoRu_2Al_5$ composition exhibits no anomaly indicating ferromagnetism. Therefore we may consider a negligible influence of both impurity phases on magnetic properties of the sample. The main phase was found to be well homogeneous over the sample (with a resolution of about 1 μm).

Lattice parameters of samples representing the parent compounds UCoAl and URuAl, have been found to be in good agreement with the literature data. Figure 2 shows the concentration dependence of lattice parameters. Since the difference between the lattice parameters of the parent compounds is rather small (less than 3% for a and less than 2% for c), a linear concentration dependence could be expected in solid solution. In fact, we have observed pronounced deviations from linearity, positive for a and negative for c. This leads to strong decrease in the c/a ratio with x at low Ru contents and a slow increase for Ru-rich compounds yielding a c/a minimum at around $x = 0\cdot6$ (fig. 2). In spite of these anomalies, the unit-cell volume V obeys satisfactorily Vegard's law (fig. 2), in accordance with the larger atomic radius of Ru (134 pm) than of Co (125 pm).

Similar behaviour of lattice parameters has been observed also in other $UT'_{1-x}T''_xX$ systems, namely in $UNi_{1-x}Fe_xAl$, $UCo_{1-x}Fe_xAl$ (Troć 1986, Troć *et al.* 1995) and $UCo_{1-x}Ru_xSn$ (Andreev *et al.* 1995b). The nonlinearity was explained by a non-statistical occupation of the two non-equivalent lattice positions (T_1 and T_2) by the transition-metal atoms. When inspecting fig. 1, we see that the T_1 position is surrounded by three U atoms in the same basal plane and six X atoms from nearest layers, whereas T_2 and has three X neighbours in plane and six U neighbours from nearest layers. Using atomic coordinates for UCoAl obtained by the neutron diffraction measurements on a single crystal (Wulff *et al.* 1990), one can find that the U–Co_1 and U–Co_2 distances are almost equal (281 and 282 pm respectively) and correspond well to the sum of atomic radii of U and Co (281 pm). However, the Al–Co_1 distance (254 pm) is shorter than the Al–Co_2 spacing (262 pm). An analogous correlation holds also for URuAl, where the U–Ru_1 spacing is 290 pm and the U–Ru_2 spacing is 289 pm ($R_U + R_{Ru} = 290$ pm), whereas for Al–Ru_1 this is 259 pm and for Al–Ru_2 270 pm (derived from single-crystal neutron diffraction data (Paixão *et al.* 1994)). Therefore, if the site occupation is not statistical, atoms of larger radius are expected to occupy preferentially the T_2 sites. Such a preferential occupation has actually been found by Mössbauer effect studies of the $UNi_{1-x}Fe_xAl$ system. The preference in occupation is not perfect but rather well pronounced (Troć *et al.* 1995).

Fig. 2

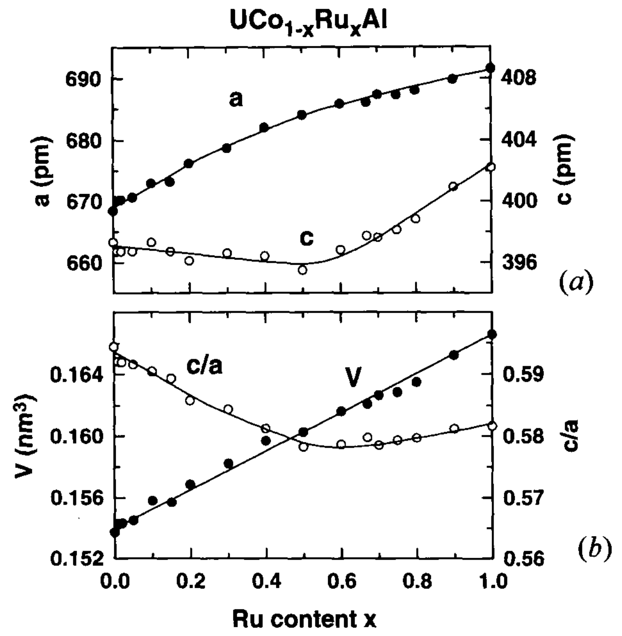

Concentration dependences of (*a*) the lattice parameters *a* and *c* and (*b*) their ratio *c*/*a* and the unit-cell volume *V*.

By analogy, we could expect that in the $UCo_{1-x}Ru_xAl$ system the Ru atoms occupy preferentially the T_2 position.

It should be mentioned, however, that the Al–Co distances in UCoAl and the Al–Ru distances in URuAl are considerably shorter (by about 12%) than the sums of corresponding atomic radii ($R_{Al} + R_{Co} = 268$ pm; $R_{Al} + R_{Ru} = 277$ pm). This shows that we could not be sure about the above speculations on the preference in occupation, based on a close-packed model, especially taking into account that the minimum in $c(x)$ and the change in slope of $a(x)$ do not appear at $x = \frac{2}{3}$. Moreover, similar non-monotonic behaviour of the lattice parameters was observed also in the $UCoAl_{1-x}Sn_x$ system where the substitution involves only one equivalent position of the X atoms (Andreev *et al.* 1996). At least small single crystals are desirable to determine the site occupation factors for Co and Ru over T_1 and T_2 positions by an X-ray study.

The shortest distance $d_{U\text{-}U}$ between the nearest U atoms in UTX compounds with the ZrNiAl structure is equal to 0·52*a* (four such neighbours in the basal plane). In UCoAl and URuAl, $d_{U\text{-}U} = 347$ pm and $d_{U\text{-}U} = 359$ pm respectively. The next inter-uranium distance (along the *c* axis) exceeds $d_{U\text{-}U}$ by about 12%. Although the contraction of the lattice along the *c* axis together with the pronounced expansion within the basal plane for $x \leqslant 0{\cdot}5$ result in a significant reduction in the *c*/*a* ratio (fig. 2), nearest U neighbours are always found in the basal plane.

3.2. *Ground-state magnetic properties*

The low-field part of magnetization curves with hysteresis loops after application of a 10 T pulse field at 4·2 K are presented in fig. 3 for selected compounds, while

Fig. 3

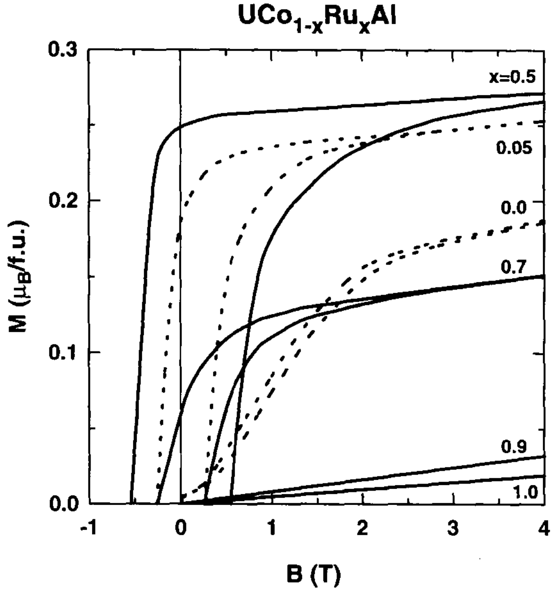

Low-field part of magnetization curves with hysteresis loops after application of a 10 T pulse field at 4·2 K.

fig. 4 shows the high-field magnetization curves (obtained with a decreasing field). The broken lines in fig. 4 represent the extrapolations of high-field curves to zero field, from which the spontaneous moment was determined. Three kinds of magnetic behaviour can be distinguished in figs. 3 and 4.

(*a*) Paramagnetism occurs in compounds with the highest Ru content ($x > 0{\cdot}75$; $x = 0{\cdot}9$ and 1·0 in figs. 3 and 4), with linear magnetization curves up to 10 T.

(*b*) Paramagnetic UCoAl has a broad metamagnetic transition around 0·8 T. The remanent magnetic moment of 0·01μ_B manifests a tiny ferromagnetic contribution (depending on deviations from 1 : 1 : 1 stoichiometry, it may vary between zero and 0·1μ_B (Andreev 1990)). This curve of M against B agrees well with the c-axis single-crystal data (Sechovsky *et al.* 1986, Andreev 1990). The polycrystalline results show obviously a broader transition and smaller (half the size of that for the single-crystal results) magnetization jump across the transition, which is due to the uniaxial anisotropy in UCoAl.

(*c*) Ferromagnetism already appears for very low Ru content and persists up to $x \approx 0{\cdot}75$; for further analysis we consider that in materials with uniaxial anisotropy the spontaneous magnetic moment derived from the polycrystalline data is 0·5 of the easy-axis spontaneous moment. The concentration dependence of μ_s is presented in fig. 5. It has a broad maximum around $x = 0{\cdot}3$, where μ_s reaches 0·6μ_B, which compares with that for UCoGa (Andreev *et al.* 1984a,b), but also with the saturated moment of UCoAl itself derived from magnetization at 35 T (Sechovsky *et al.* 1986).

Fig. 4

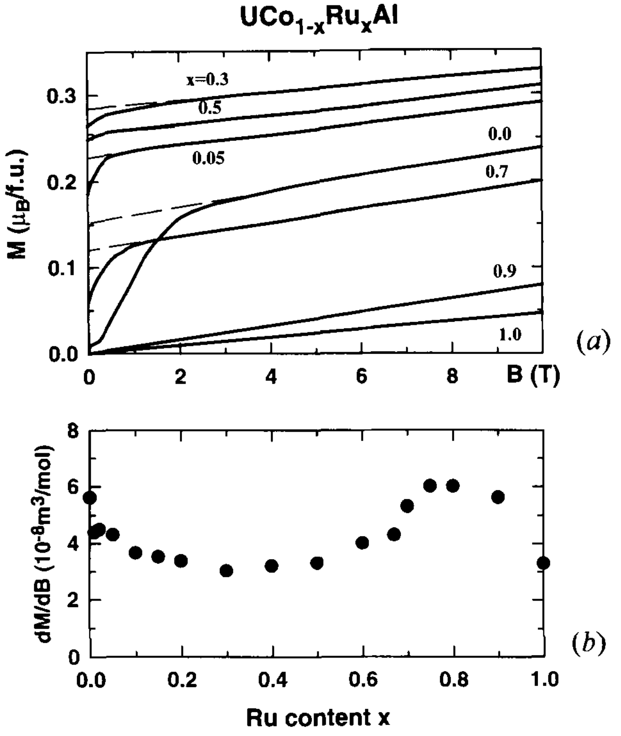

(*a*) High-field magnetization curves (field-down branch) at 4·2 K. The broken lines represent the extrapolations of high-field curves to zero field. (*b*) Concentration dependence of the high-field (10 T) differential susceptibility at 4·2 K.

UCoAl exhibits a very large high-field susceptibility in the easy-magnetization direction even above the metamagnetic transition, which may be related to the instability of the magnetic moment (Sechovsky *et al.* 1986). Figure 4 shows the dependence of the high-field susceptibility (at 10 T) on the Ru content. The onset of ferromagnetism at $x = 0{\cdot}01$ stabilizes the magnetic moment, and the high-field suceptibility immediately decreases, reaching a broad minimum around $x = 0{\cdot}3$, which corresponds to compounds with the maximum spontaneous moment. In this range, the high-field susceptibility of the polycrystal reflects mainly the magnetic anisotropy.

In compounds with $x > 0{\cdot}5$, the high-field susceptibility starts to increase and reaches its maximum in the vicinity of $x = 0{\cdot}8$, which corresponds to the disappearance of ferromagnetism.

3.3. *Concentration and temperature dependence of ferromagnetism*

Figure 6 represents the temperature dependence of the ac magnetic susceptibility for selected $UCo_{1-x}Ru_xAl$ compounds. For $x = 0$, there is no anomaly indicating magnetic ordering, in agreement with the paramagnetic ground state of UCoAl. In accordance with the magnetization results, the substitution of only 1 at.% Ru for Co leads to ferromagnetic ordering which is indicated by a maximum in the curve of χ_{ac}

Fig. 5

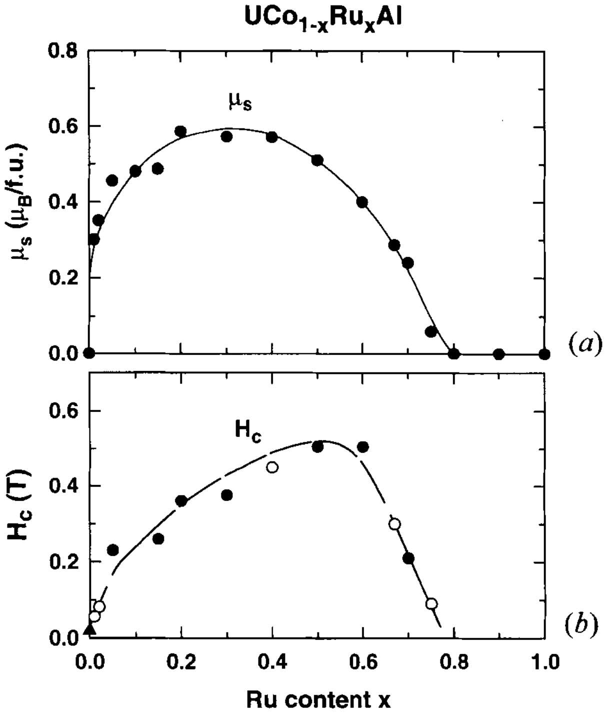

Concentration dependences of (*a*) the spontaneous magnetic moment μ_s and (*b*) the coercive field H_c at 4·2 K. For $H_c(x)$, the full circles correspond to the pulsed field, and the open circles to the steady field. For UCoAl, the half-width of hysteresis at metamagnetic transition is shown as a full triangle.

against T. With increasing Ru content, the maximum becomes sharper and moves to higher temperatures. The sharp maximum observed on the curve of χ_{ac} against T observed for $0{\cdot}05 \leqslant x \leqslant 0{\cdot}4$ is typical for ferromagnetic UTX compounds, where T_C can be easily determined from χ_{ac} data and its value coincides with that derived from Arrott plots. On the Ru-rich side the onset of magnetic order occurs at $x = 0{\cdot}75$ where a broad maximum in the curve of χ_{ac} against T is observed (fig. 6).

The compounds with $0{\cdot}5 \leqslant x \leqslant 0{\cdot}7$ exhibit an additional feature, namely a second maximum on the curve of χ_{ac} against T (fig. 7). The appearance of a second maximum may indicate an additional magnetic phase transition in the ordered state or can be attributed to a sudden change in the magnetization process at a certain temperature (see the discussion of magnetization curves given below) similar to that observed in UCoGa (Nakotte *et al.* 1993). We cannot also exclude that it is due to structural inhomogeneities on the atomic level (clusters) which may appear in solid solutions. Considering results of microprobe analysis of $UCo_{0{\cdot}33}Ru_{0{\cdot}67}Al$, which belongs to this composition range, we can exclude any inhomogeneity on a larger scale.

Magnetization isotherms of $UCo_{0{\cdot}99}Ru_{0{\cdot}01}Al$ measured in steady fields are presented in fig. 8. They display behaviour of a typical ferromagnet. Figure 8 also shows

Fig. 6

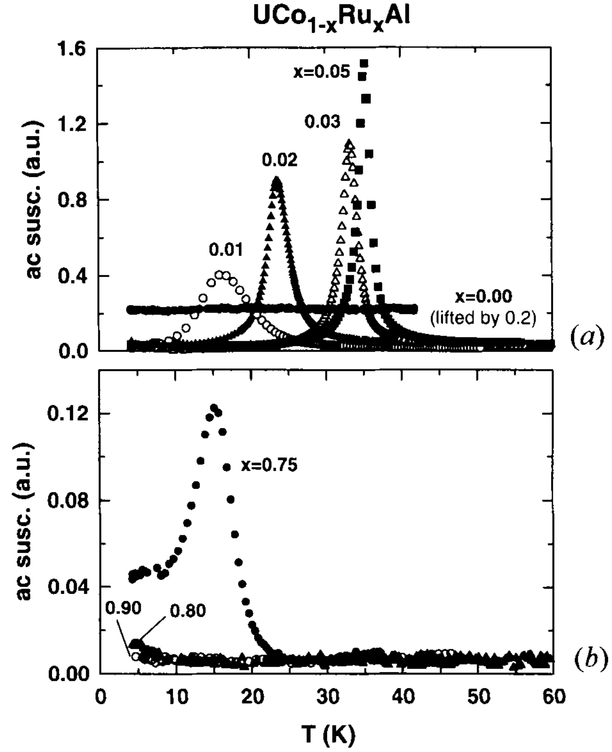

Temperature dependences of the ac magnetic susceptibility of compounds (*a*) with low Ru content and (*b*) with high Ru content (a.u., arbitrary units).

the Arrott plots for this compound. The T_C value found from these data is 21 K which corresponds well to the inflection point on the decreasing side of the ac susceptibility maximum. Very similar results (with $T_C = 26$ K) are obtained for $x = 0\cdot02$. The temperature dependences of the magnetic moment in a constant field for several representative compounds illustrating their ferromagnetic behaviour are shown in fig. 9. There is a clear difference from the paramagnet UCoAl, for which the single-crystal results are presented in the inset in fig. 9.

While the onset of ferromagnetism on the Co-rich side of the UCo$_{1-x}$Ru$_x$Al system immediately leads to normal ferromagnet features, the magnetic behaviour of analogous Ru-rich compounds differs qualitatively. Magnetization isotherms and corresponding Arrott plots for UCo$_{0\cdot25}$Ru$_{0\cdot75}$Al, the first ferromagnet from the URuAl side of the system are shown in fig. 10. If in UCo$_{0\cdot99}$Ru$_{0\cdot01}$Al the development from the low-temperature ferromagnetic curve to paramagnetic straight line arises because of a decrease in spontaneous moment with a simultaneous increase in high-field susceptibility (fig. 8), in UCo$_{0\cdot25}$Ru$_{0\cdot75}$Al the slope of the isotherms varies weakly with temperature and remains high even at low temperatures. A first glance at the Arrott plots then might lead to the conclusion that the compound has no spontaneous moment at all down to 2 K. However, the remanent magnetization and hysteresis are observed up to 35 K which shows the importance of inspecting the low-field parts of Arrott plots.

Fig. 7

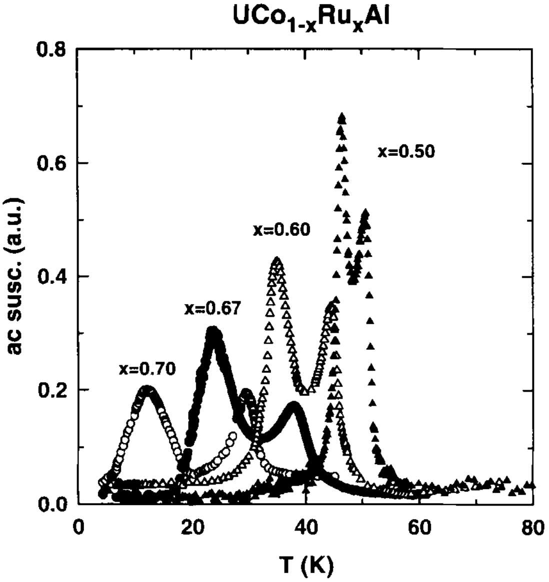

Temperature dependences of the ac magnetic susceptibility of compounds showing two maxima (a.u., arbitrary units).

Such behaviour can be considered in two ways. A more conventional explanation may be based on magnetic inhomogeneities on a microscopic scale induced by substitutions, that is the coexistence of ferromagnetic clusters and paramagnetic regions with strongly enhanced susceptibility. An explanation considering a magnetically homogenous sample in a low-moment ferromagnetic ground state may also be plausible. The strong increase in the magnetic moment over a wide range of magnetic fields can then be attributed to a broad transition to the high-moment state. As a variant of this picture a spontaneous uncompensated antiferromagnetic state which is gradually transforming under a magnetic field into the ferromagnetic state may be considered.

Magnetization isotherms and Arrott plots for the compound from the concentration range with two maximum in the ac susceptibility, $UCo_{0\cdot33}Ru_{0\cdot67}Al$, are presented in fig. 11. Their inspection offers a contradictory picture which is analogous to $UCo_{0\cdot25}Ru_{0\cdot75}Al$. An ordering temperature of 32 K may be derived from the high-field part of Arrott plots, but the $M(B)$ curves at 35 K clearly manifests a spontaneous moment. The low-field isotherms at 24–50 K presented in fig. 12 show hysteresis and, consequently, ferromagnetism far above 32 K. The temperature dependence of the spontaneous magnetic moment (determined from the low-field range), ac susceptibility and coercive field are collected in fig. 12 (*b*). It is seen that the inflection point of the descending side of the maximum of $\chi_{ac}(T)$ corresponds roughly to the end of a sharp decrease in H_c and to the inflection point in $\mu_s(T)$. We can propose that the phase transition occurs at about 30 K from the ferromagnet (below 30 K) to one of possible states discussed for the $UCo_{0\cdot25}Ru_{0\cdot75}Al$ sample (above). Similar behaviour is seen in fig. 9 for the compound with $x = 0{\cdot}6$. The $\mu(T)$ curve has an inflection at 38 K and it corresponds well to loss of thermomagnetic hysteresis. A less

Fig. 8

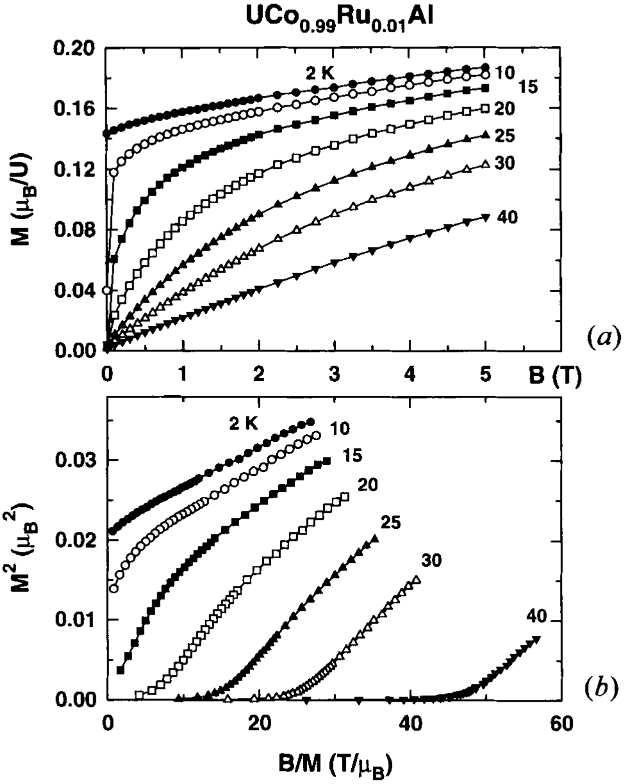

(*a*) Magnetization isotherms and (*b*) Arrott plots for $UCo_{0\cdot99}Ru_{0\cdot01}Al$.

Fig. 9

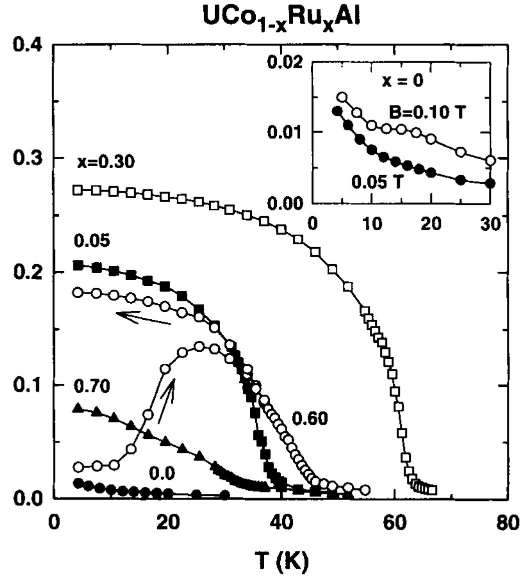

Temperature dependences of the magnetic moment in 0·05 T field for several compounds. The measurements were done on the field-cooled samples. For $x = 0{\cdot}6$, the thermomagnetic hysteresis is also shown. The inset shows results for a UCoAl single crystal along the *c* axis.

Fig. 10

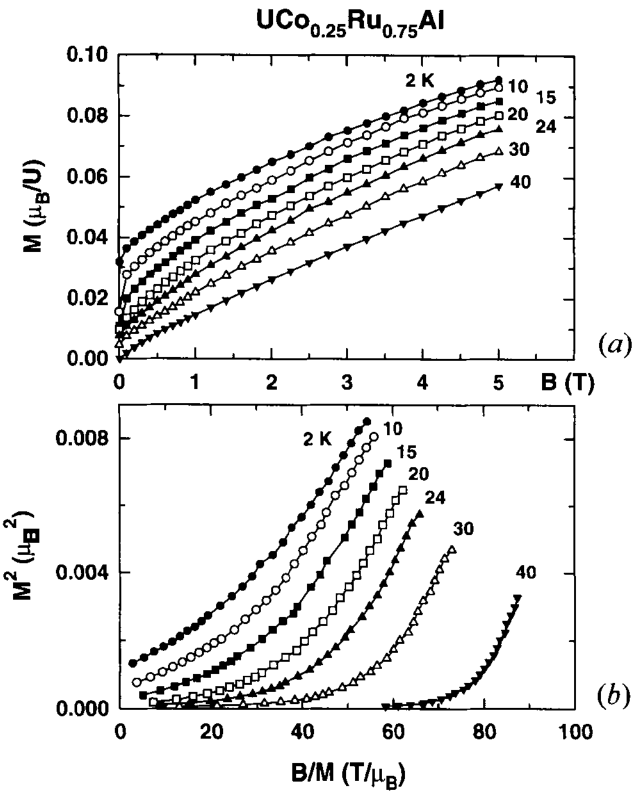

(*a*) Magnetization isotherms and (*b*) Arrott plots for $UCo_{0.25}Ru_{0.75}Al$.

pronounced but still visible inflection is 18 K on the $\mu(T)$ curve for $x = 0.70$ (fig. 9) is also in a good agreement with the ac susceptibility data.

3.4. *Paramagnetic susceptibility*

The temperature dependence of the magnetic susceptibility above 70 K measured for all $UCo_{1-x}Ru_xAl$ compounds obeys the modified Curie–Weiss law with a temperature-independent term $\chi_0 \approx 1 \times 10^{-8}$ m^3 mol^{-1}. The concentration dependence of the paramagnetic Curie temperature Θ_p presented in fig. 13 shows features analogous to the behaviour of the $URh_{1-x}Ru_xAl$ compounds (Sechovsky *et al.* 1992). The values of the effective magnetic moment μ_{eff} derived from polycrystalline susceptibility data have no real physical meaning for systems with strong magnetic anisotropy in the paramagnetic state. The increase in μ_{eff} with increasing x observed for Ru-rich compounds (fig. 13) seems to be significant however.

The low-temperature susceptibility of URuAl (fig. 14) shows a broad maximum at 50 K, indicating spin fluctuation behaviour. The Co substitution for Ru produces effects analogous to the Rh doping (Sechovsky *et al.* 1992), in particular, pushing the maximum to lower temperatures and inducing a low-temperature upturn. The susceptibility behaviour for $UCo_{0.20}Ru_{0.80}Al$ indicates proximity of ferromagnetism at low temperatures.

Fig. 11

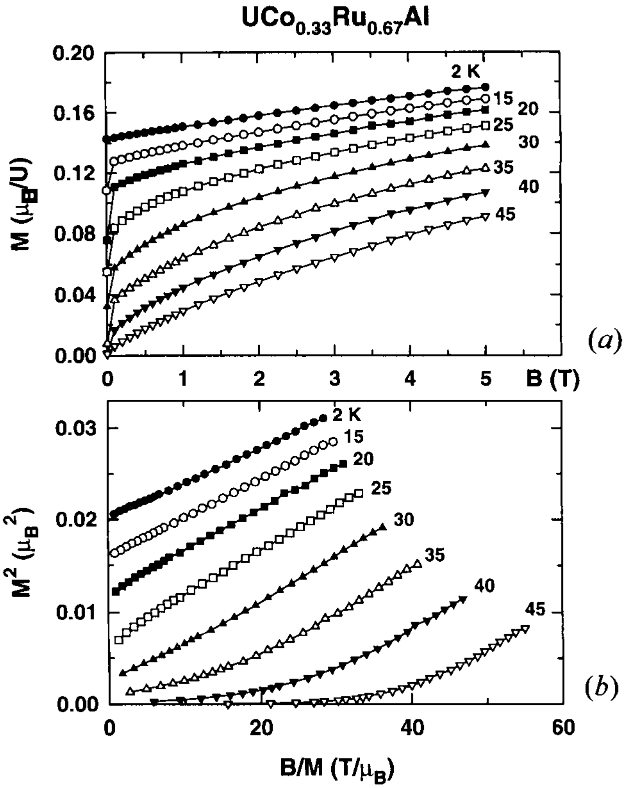

(*a*) Magnetization isotherms and (*b*) Arrott plots for $UCo_{0\cdot33}Ru_{0\cdot67}Al$.

3.5. *How can the development of magnetism in the* $UCo_{1-x}Ru_xAl$ *system be understood?*

Figure 15 shows the x–T magnetic phase diagram which we have constructed after analysis of the above-discussed results. The bell-shaped $T_C(x)$ dependence is rather similar to the concentration dependence of the magnetic moment (fig. 5). In a broad maximum around $x = 0{\cdot}3$–$0{\cdot}4$, T_C reaches 60 K.

Both the parent compounds of this system, UCoAl and URuAl, have a paramagnetic ground state. Therefore it might be surprising that their solid solutions become ferromagnetic for a wide concentration range. An analogy on the Ru-rich side can be found in the $URh_{1-x}Ru_xAl$ compounds (Sechovsky *et al.* 1992), where Rh substitutions for Ru lead to a ferromagnetic state for a comparable x value. It is interesting to considering that Rh and Co have approximately the same population of 4d and 3d band states respectively. Nevertheless, the onset of ferromagnetism in the $URh_{1-x}Ru_xAl$ system is natural because URhAl itself is a ferromagnet, but here also we observe a maximum in the concentration dependence of T_C, which indicates a somewhat closer relationship beween the $URh_{1-x}Ru_xAl$ and $UCo_{1-x}Ru_xAl$ systems. To complete the information file we should mention that ferromagnetism appears for an even lower Ni doping in the URuAl than in the case of the Co (or Rh) doping. Naturally, T_C against x in the $UNi_{1-x}Ru_xAl$ system exhibits also a

Fig. 12

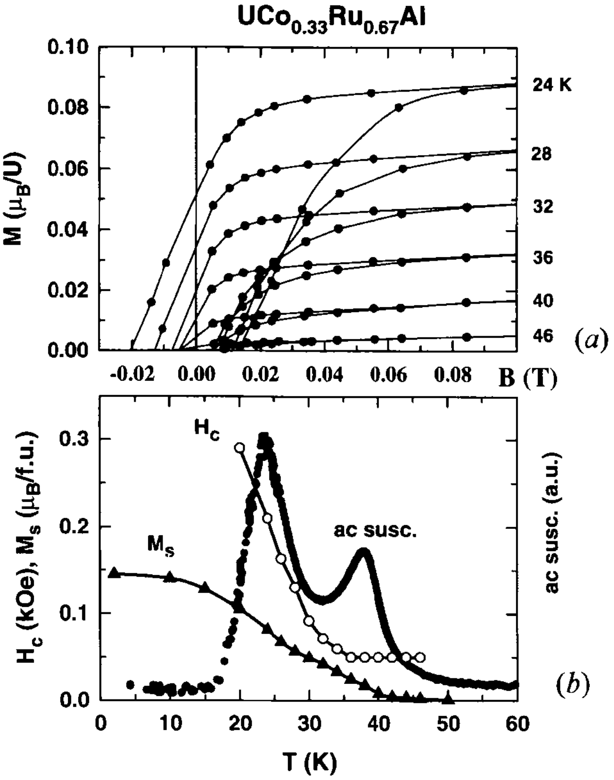

(*a*) Low-field magnetization isotherms at 24–46 K and (*b*) temperature dependences of the spontaneous magnetic moment μ_S, ac susceptibility and coercive field H_c for $UCo_{0\cdot33}Ru_{0\cdot67}Al$ (a.u., arbitrary units).

maximum for intermediate concentration and ferromagnetism disappears for high Ni concentrations (in $UNi_{0\cdot85}Ru_{0\cdot15}Al$). UNiAl itself and compounds with $x < 0\cdot15$ are antiferromagnetic (Andreev *et al.* 1997) (results of detailed study will be published elsewhere).

At this moment we may try to consider a simple model, which would account for all these ‘striking’ results, which seem to break the standard picture of the development of magnetism in UTX ternaries of the ZrNiAl structure, mentioned in § 1. As the prominent mechanisms affecting the size of U magnetic moments and their ordering, the overlap of the 5f wavefunctions of neighbouring U atoms and the hybridization of the U 5f states with the s,p,d valence states of ligands (T and X atoms) should be considered. Both mechanisms induce two important effects in actinide compounds: firstly delocalization of the U 5f states, leading ultimately to wash-out of the magnetic moments, and secondly exchange interactions correlating the U 5f magnetic moments via direct 5f–5f and indirect exchange involving non-f states.

It is evident already from the structure consideration that these effects are strongly anisotropic in the ZrNiAl-structure family. The close packing of U and T atoms in the basal plane probably results in both a non-negligible 5f–5f overlap and

Fig. 13

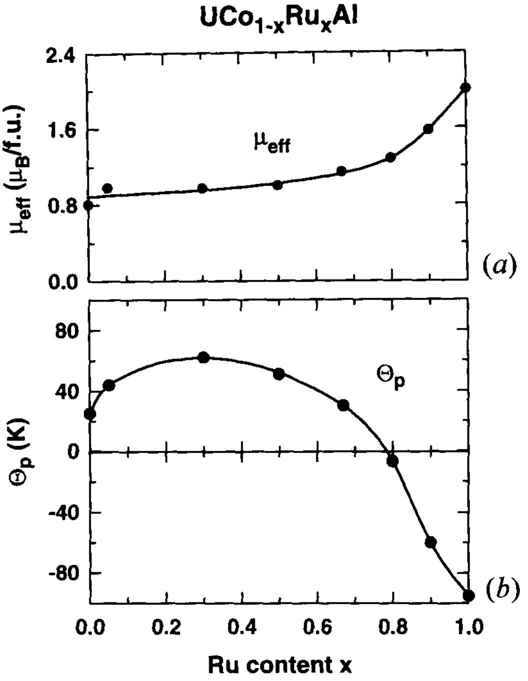

Concentration dependences of (*a*) the effective magnetic moment μ_{eff} and (*b*) the paramagnetic Curie temperature Θ_p.

a strong 5f–d hybridization involving the transition metal d states, which compresses the 5f charge density towards the basal plane. Since the 5f states with strong spin–orbit interaction promote orbital magnetic moments, which are indeed observed experimentally (for example Wulff *et al.* (1990)), a strong uniaxial anisotropy with magnetic moments locked along the *c* axis is an inevitable element of magnetism leading to Ising-like systems. Another consequence of the 5f–5f overlap and the 5f–d hybridization within the basal plane is a strong ferromagnetic coupling of the U magnetic moments involved. This situation leads to magnetic structures built up of ferromagnetic basal-plane layers.

Inspecting the crystal structure, we may deduce that along the *c* axis both 5f–d (U–T) and 5f–3p (U–Al) hybridization should be considered. The first type should dominate for earlier d elements (Ru), whereas it ceases with additional filling of the d shell, leaving the 5f–3p hybridization channel gradually more important. We may speculate that the former type leads preferably to a ferromagnetic type of U–U coupling along *c*, whereas the latter tends to an antiferromagnetic type of coupling.

Starting from URuAl, the 5f–d hybridization becomes reduced when partly substituting Rh, Co or Ni for Ru, which allows formation of the U 5f magnetic moments (coupled ferromagnetically within the basal plane) for a certain concentration of the substituent, but the moments are relatively small and the interaction along *c* is ferromagnetic. When proceeding with the substitution further, the U moments increase in magnitude, but the coupling along *c* weakens, and finally

Fig. 14

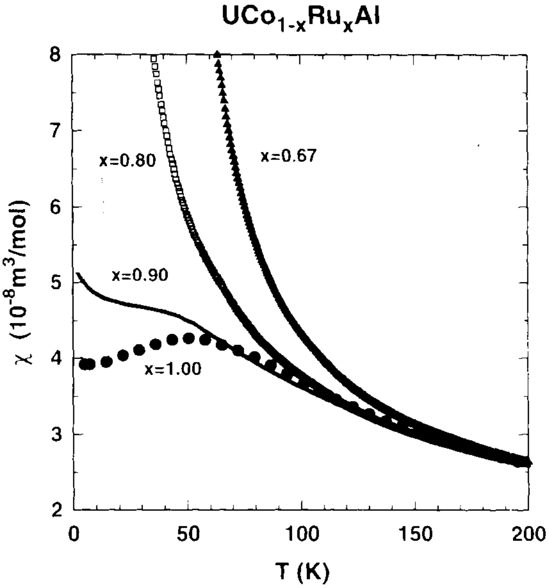

Temperature dependence of the magnetic susceptibility χ for compounds with a high Ru content.

Fig. 15

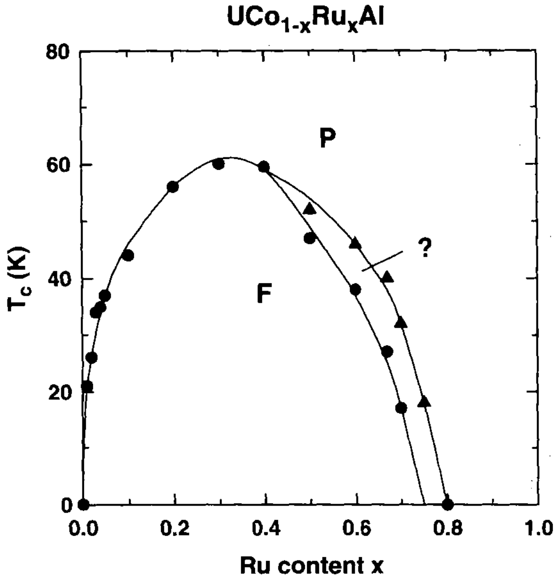

Magnetic x–T phase diagram of the $UCo_{1-x}Ru_xAl$ system.

upon the decay of 5f–d exchange polarization the 5f–3p channel overtakes the dominance, leading to relatively weak antiferromagnetic coupling along *c*. Thus the reduction in the exchange coupling along *c* leads to a final decay in the ordering temperature, despite the fact that strong coupling along the other two dimensions persists.

The fact that not only the strength of the hybridization but also the U–U exchange interaction as the second-order effect, can influence the magnitude of the U moments can be deduced from the non-magnetic ground state of UCoAl. This compound represents in the framework of our simple model a delicate balance of ferromagnetic and antiferromagnetic components of the exchange interaction along *c*. It would be interesting to see whether the existence of the two non-contiguous regions, one ferromagnetic and the other antiferromagnetic, occur more generally in pseudoternary UTX compound at least with the ZrNiAl structure type. Generally the frustration in itinerant system can suppress local moments (as for example in $REMn_2$ compounds (Ballou *et al.* 1991)) and the importance of the intersite exchange interaction for the moment stability has also been demonstrated recently for f systems (Krishnamurthy *et al.* 1995). It is interesting to compare the case of UCoAl with a less delocalized counterpart UNiGa, in which weak competing interactions along *c* lead to a complex stacking of U moments (Prokeš *et al.* 1996).

We are aware that a possible preferential occupation of T_1 or T_2 sites by the substituent atoms may substantially influence this picture. Therefore extensive neutron diffraction studies are being scheduled to focus on this issue and also on the possible non-uniform ferromagnetic structure in the temperature region between the two ac susceptibility peaks.

§ 4. Conclusions

In conclusion we have observed ferromagnetism for a wide concentration range of solid solutions of UCoAl and URuAl, two compounds with a paramagnetic ground state. For the development of magnetism in this quasiternary series a simple model is proposed assessing components of the anisotropic 5f–ligand hybridization and the hybridization-induced exchange interaction. The proper theoretical background for the hybridization-induced two-ion exchange interaction is being constantly developed by Hu and Cooper (1993). *Ab-initio* calculations using this approach are strongly desirable to explain the intriguing magnetic properties of UTX compounds.

Acknowledgements

The work was supported by Grant No. A1010614 of the Grant Agency of the Academy of Sciences of the Czech Republic and Grant No. 202/96/0207 of the Grant Agency of the Czech Republic.

References

Andreev, A. V., 1990, *Phys. Metals Metallogr* (USSR), **69**, 68.

Andreev, A. V., Aruga Katori, H., and Goto, T., 1995a, *J. Alloys Compounds*, **224**, 117.

Andreev, A. V., Aruga Katori, H., Goto, T., Sechovsky, V., and Havela, L., 1995b, *J. Magn. magn. Mater.*, **140–144**, 1383.

Andreev, A. V., and Bartashevich, M. I., 1986, *Phys. Metals Metallogr. (USSR)*, **62**, 50.

Andreev, A. V., Deryagin, A. V., and Yumaguzhin, R. Yu., 1984a, *Soviet Phys. JETP*, **59**, 1082.

ANDREEV, A. V., HAVELA, L., SECHOVSKY, V., ARUGA KATORI, H., and GOTO, T., 1996, *J. Alloys Compounds*, **235**, 72.

ANDREEV, A. V., HAVELA, L., ZELENY, M., and HREBIK, J., 1984b, *Phys. Stat. sol.* (a), **82**, 191.

ANDREEV, A. V., LEVITIN, R. Z., POPOV, YU. F., and YUMAGUZHIN, R. YU., 1985, *Soviet Phys. Solid St.*, **27**, 1145.

ANDREEV, A. V., SECHOVSKÝ, V., HAVELA, L., BARTASHEVICH, M. I., GOTO, T., DREMOV, R. V. and KOZLOVSKAYA, I. K., 1997, *Physica* B (to be published).

BALLOU, R., LACROIX, C., and NUNEZ-REGUEIRO, M. D., 1991, *Phys. Rev. Lett.*, **66**, 1910.

ERIKSSON, O., JOHANSSON, B., and BROOKS, M. S. S., 1989, *J. Phys. condens. Matter*, **1**, 4005.

HAVELA, L., HREBIK, J., ZELENY, M., and ANDREEV, A. V., 1985, *Acta Phys. Polonica* A, **68**, 493.

HU, G.-J., COOPER, B. R., 1993, *Phys. Rev.* B, **48**, 12 743.

KRISHNAMURTHY, V. V., MISHRA, S. N., PRESS, M. R., and DEVARE, S. H., 1995, *Phys. Rev. Lett.*, **74**, 1661.

MOROZKIN, A. V., and SEROPEGIN, YU. D., 1996, *J. Alloys Compounds*, **237**, 124.

NAKOTTE, H., DE BOER, F. R., HAVELA, L., SVOBODA, P., SECHOVSKY, V., KERGADALLAN, Y., SPIRLET, J. C., and REBIZANT, J., 1993, *J. appl. Phys.*, **73**, 6554.

PAIXÃO, J. A., DELAPALME, A., PAULUS, W., and BRÜCK, E., 1994, *Z. Kristallogr.*, **209**, 594.

PALSTRA, T. T. M., 1986, PhD Thesis, University of Leiden.

PROKEŠ, K., BRÜCK, E., DE BOER, F. R., MIHÁLIK, M., MENOVSKY, A., BURLET, P., MIGNOT, J. M., HAVELA, L., and SECHOVSKÝ, V., 1996, *J. appl. Phys.*, **79**, 6396.

SECHOVSKY, V., and HAVELA, L., 1988, *Intermetallic Compounds of Actinides*, Ferromagnetic Materials, Vol. 4, edited by E. P. Wohlfarth and K. H. J. Buschow (Amsterdam: North-Holland), p. 309.

SECHOVSKY, V., HAVELA, L., DE BOER, F. R., FRANSE, J. J. M., VEENHUIZEN, P. A., SEBEK, J., STEHNO, J., and ANDREEV, A. V., 1986, *Physica* B, **142**, 283.

SECHOVSKY, V., HAVELA, L., DE BOER, F. R., VEENHUIZEN, P. A., SUGIYAMA, K., KURODA, T., SUGIURA, E., ONO, M., DATE, M., and YAMAGISHI, A., 1992, *Physica* B, **177**, 164.

TROĆ, R., 1986, *Digest of the 16 Journées des Actinides*, Eibsee, 1986, p. 39.

TROĆ, R., TRAN, V. H., VAGIZOV, F. G., and DRULIS, H., 1995, *Phys. Rev.* B, **51**, 3003.

VEENHUIZEN, P. A., DE BOER, F. R., MENOVSKY, A. A., SECHOVSKY, V., and HAVELA, L., 1988, *J. Phys.*, Paris, **49**, C8–485.

WULFF, M., FOURNIER, J.-M., DELAPALME, A., GILLON, B., SECHOVSKY, V., HAVELA, L., and ANDREEV, A. V., 1990, *Physica* B, **163**, 331.

ZOGAL, O. J., LAM, D. J., ZYGMUNT, A., DRULIS, H., PETRYNSKI, W., and STALINSKI, S., 1984, *Phys. Rev.* B, **28**, 4837.